Approximate analytical formulation of radial diffusion and whistler-induced losses from a preexisting flux peak in the plasmasphere

D Mourenas, A.V. Artemyev, O. V. Agapitov

AGU PUBLICATIONS

JGR

Journal of Geophysical Research: Space Physics

RESEARCH ARTICLE
10.1002/2015JA021623

Key Points:
- Approximate analytical model of radial diffusion from a narrow flux peak at low L
- Investigation of potential access of relativistic electrons to the inner belt
- Could allow easy parametric studies of radial diffusion from a flux peak inside the plasmasphere

Correspondence to:
D. Mourenas,
didier.mourenas@gmail.com

Citation:
Mourenas, D., A. V. Artemyev, and O. V. Agapitov (2015), Approximate analytical formulation of radial diffusion and whistler-induced losses from a preexisting flux peak in the plasmasphere, *J. Geophys. Res. Space Physics*, *120*, 7191–7208, doi:10.1002/2015JA021623.

Received 25 JUN 2015
Accepted 5 AUG 2015
Accepted article online 7 AUG 2015
Published online 5 SEP 2015

Approximate analytical formulation of radial diffusion and whistler-induced losses from a preexisting flux peak in the plasmasphere

D. Mourenas[1], A. V. Artemyev[2], and O. V. Agapitov[3,4]

[1]CEA, DAM, DIF, Arpajon, France, [2]LPC2E/CNRS, University of Orleans, Orleans, France, [3]Space Science Laboratory, University of California, Berkeley, California, USA, [4]National Taras Shevchenko University of Kiev, Kiev, Ukraine

Abstract Modeling the spatiotemporal evolution of relativistic electron fluxes trapped in the Earth's radiation belts in the presence of radial diffusion coupled with wave-induced losses should address one important question: how deep can relativistic electrons penetrate into the inner magnetosphere? However, a full modeling requires extensive numerical simulations solving the comprehensive quasi-linear equations describing pitch angle and radial diffusion of the electron distribution, making it rather difficult to perform parametric studies of the flux behavior. Here we consider the particular situation where a localized flux peak (or storage ring) has been produced at low $L < 4$ during a period of strong disturbances, through a combination of chorus-induced energy diffusion (or direct injection) at low L together with enhanced wave-induced losses and outward radial transport at higher L. Assuming that radial diffusion can be further described as the spatial broadening within the plasmasphere of this preexisting flux peak, simple approximate analytical solutions for the distribution of trapped relativistic electrons are derived. Such a simplified formalism provides a convenient means for easily determining whether radial diffusion actually prevails over atmospheric losses at any particular time for given electron energy E and location L. It is further used to infer favorable conditions for relativistic electron access to the inner belt, providing an explanation for the relative scarcity of such a feat under most circumstances. Comparisons with electron flux measurements on board the Van Allen Probes show a reasonable agreement between a few weeks and 4 months after the formation of a flux peak.

1. Introduction

The spatiotemporal evolution of relativistic electron fluxes trapped in the Earth's radiation belts has been a topic of intense research in the past decades, partly due to the threat that such killer particles pose to sensitive electronic components of satellites. Indeed, trapped energetic electron fluxes are known to vary strongly with geomagnetic activity. As a result, space weather disturbances can affect the reliability of spaceborne technological systems via total radiation doses and displacement damages due to MeV electrons as well as via charging effects related to lower energy electrons [e.g., see *Gubby and Evans*, 2002; *Horne et al.*, 2013].

Very sharp and localized increases of highly relativistic electron flux are frequently observed during strong geomagnetic storms [e.g., see *Horne et al.*, 2005; *Shprits et al.*, 2006; *Baker et al.*, 2013; *Thorne et al.*, 2013a, 2013b; *Zhao and Li*, 2013a; *Li et al.*, 2014a, and references therein]. Such dramatic increases are mainly due to quasi-linear electron acceleration by intense whistler-mode chorus waves present just outside the eroded plasmasphere [e.g., see *Horne et al.*, 2005; *Shprits et al.*, 2006; *Li et al.*, 2006; *Thorne et al.*, 2013b; *Kellerman et al.*, 2014; *Li et al.*, 2014a, and references therein], interplanetary shock interaction with the Earth's magnetosphere [*Blake et al.*, 1992; *Li et al.*, 1993], or acceleration due to inward radial diffusion [*Li et al.*, 2001, 2006; *Gabrielse et al.*, 2012], combined with dropouts or losses due to wave-particle interactions at farther distances $L = R_0/R_E$ (with L McIlwain's number, R_0 the equatorial distance to the center of the Earth, and R_E the Earth's radius) outside a recovering plasmasphere, sometimes during a consecutive secondary storm [*Turner et al.*, 2012; *Shprits et al.*, 2013; *Kellerman et al.*, 2014; *Ukhorskiy et al.*, 2015]. The strong rise of the intensity of whistler-mode waves during disturbed periods can increase both the energization of electrons and their losses to the atmosphere via pitch angle scattering toward the loss cone [*Kennel and Petschek*, 1966; *Lyons et al.*, 1972; *Thorne*, 2010; *Agapitov et al.*, 2014]. Radial diffusion of electrons induced by ULF fields has also been shown to depend strongly on geomagnetic activity index K_p [*Schulz and Lanzerotti*, 1974; *Brautigam and Albert*, 2000;

Shprits et al., 2008; *Ozeke et al.*, 2014]. Alternatively, a localized flux peak of relativistic electrons may also be formed artificially, e.g., in the aftermath of a high-altitude nuclear test, as it happened in 1962 [*West*, 1966].

Accurate forecasts of the evolution of the Earth's radiation belts require first to assess the relative impact of the different existing phenomena. Recent satellites have provided statistical wave models allowing to evaluate wave-induced electron losses [*Meredith et al.*, 2007, 2012; *Agapitov et al.*, 2013; *Artemyev et al.*, 2013b; *Li et al.*, 2013, 2014b; *Agapitov et al.*, 2014; *Mourenas et al.*, 2014]. Precise and detailed measurements of relativistic electron fluxes have also become available from the recently launched Van Allen Probes [e.g., *Li et al.*, 2014a; *Baker et al.*, 2014]. But due to the complexity and entanglement of the involved physical processes, any new understanding can only be obtained in general after numerous comparisons of satellite particle measurements with large-scale numerical simulations solving the Fokker-Planck diffusion equation of the trapped electron distribution [*Turner et al.*, 2012; *Thorne et al.*, 2013a; *Horne et al.*, 2013; *Li et al.*, 2014a; *Kellerman et al.*, 2014] in the presence of coupled radial diffusion and quasi-linear pitch angle and energy scattering by whistler-mode waves (of not-too-high average amplitudes, typically < 300 pT).

Much work has been done in the past to simplify the modeling of radial and pitch angle diffusion of electrons in the radiation belts [e.g., see *Lyons and Thorne*, 1973; *Schulz and Lanzerotti*, 1974; *Chiu et al.*, 1988; *Schulz*, 1991, and references therein]. Although there are already some quite precise analytical formulations for the spatiotemporal evolution of the electron distribution $f(L, t)$, they still suffer from several drawbacks. Some models are mainly numerical ones [e.g., see *Tomassian et al.*, 1972] and therefore do not provide simple analytical estimates. Similarly, the expansion of f in eigenfunctions proposed by *Schulz and Newman* [1988] to describe radial diffusion remains rather impractical, since at least 5–10 eigenfunctions must be retained in typical realistic conditions (i.e., for realistic time scales t and radial diffusion rates D_{LL} such that $D_{LL}t \sim 10^{-6} - 10^{-4}$ for $L = 1$ in the early stage of radial diffusion). In a similar vein, *Chiu et al.* [1988] have kept only five of these radial diffusion eigenfunctions (in addition to the main pitch angle one) and have attempted to infer D_{LL} and lifetimes by fitting observed electron distributions. But such a procedure remains complicated and requires a great deal of numerical computations. Moreover, keeping only five eigenfunctions makes their formulation more approximate than the full one—while corresponding already to a large number (>10) of parameters that need to be determined (at each energy): it is still far from providing really straightforward and handy analytical estimates. The employed eigenfunction decomposition for pitch angle scattering also relies on an assumption concerning the possible shapes of $D_{\alpha\alpha}(\alpha)$ [*Schulz*, 1991] that is not fully realistic [see *Mourenas et al.*, 2012b; *Artemyev et al.*, 2013a, 2013b; *Mourenas et al.*, 2015]. Nevertheless, all the above cited complex and comprehensive formulations of $f(L, t)$ can be very useful to evaluate precisely the dynamics of trapped particles in general.

In this paper, our main goal is rather to provide a much more simple and easy-to-use approximate formulation for $f(L, t)$, tailor-made for a particular set of initial conditions and making use of more realistic analytical expressions for pitch angle scattering loss. We consider the particular situation where a narrow flux peak is initially present inside the plasmasphere, and we provide rough but realistic analytical expressions describing the subsequent evolution of the relativistic electron distribution in this specific case—albeit neglecting energy diffusion, which generally abates in the aftermath of storms at lower L shells. We make use of recent approximate analytical formulations for both the radial diffusion rates [*Ozeke et al.*, 2014] and the lifetimes of relativistic electrons interacting with quasi-parallel whistler-mode waves [*Mourenas and Ripoll*, 2012; *Mourenas et al.*, 2012b; *Artemyev et al.*, 2013b, 2013a; *Mourenas et al.*, 2014] and demonstrate that the approximate analytical model allows to recover full numerical results. Next, the analytical model is compared with actual measurements performed on board the Van Allen Probes in 2012–2013, showing a good agreement. In the last section, we show that the obtained simplified analytical expressions could be useful for analyzing the evolution of measured particle distributions originating from such a preexisting flux peak. This approach allows in particular not only to easily identify phase space regions driven more by radial diffusion or atmospheric losses but also to estimate the maximum inward penetration of relativistic electrons, paving the way for parametric studies as a function of geomagnetic conditions. The obtained analytical expressions could also be used to infer radial diffusion coefficients from combined measurements of relativistic electron fluxes and hiss waves during some carefully selected periods.

2. Approximate Analytical Formulation of Radial Diffusion and Whistler-Induced Losses in the Plasmasphere

2.1. Generalities

Following previous works (e.g., see *Schulz and Lanzerotti*, [1974] especially their section III-8), we first neglect drift-shell splitting at low $L < 4$, as well as energy diffusion. The dynamics is then dominated by radial diffusion induced by ULF perturbations and losses due to quasi-linear pitch angle scattering by whistler-mode waves (toward the atmospheric loss cone). We also restrict our analysis to nearly equatorially mirroring electrons, with equatorial pitch angle $\alpha_0 \geq 70°$, which represent a major part of the trapped population inside the plasmasphere [e.g., see *Meredith et al.*, 2009; *Mourenas et al.*, 2015; *Baker et al.*, 2014]. We further assume that the effects of radial diffusion and scattering by whistler-mode waves can be considered as approximately independent, so that the full distribution can be written as $f(L,t) \sim F_\alpha(t)F_L(L,t)$, i.e., as the product of one exponentially decaying function $F_\alpha(t) = \exp(-t/\tau_L)$ weakly dependent on L representing wave-induced losses and one function $F_L(L,t)$ describing radial diffusion. This important approximation requires that the radial diffusion operator D_{LL} be only weakly dependent on α, which should apply when dealing with electrostatic perturbations but not when treating magnetic impulses [*Schulz and Lanzerotti*, 1974]. The characteristic lifetime τ_L of electrons associated to pitch angle scattering by whistler-mode waves [*Lyons et al.*, 1972] is also required to be weakly dependent on L. These two important requirements will be further checked below. Then, building on the fact that the variable $\zeta = M/\sin^2\alpha \sim M$ (with $M = p^2\sin^2\alpha/(2m_eB)$ the first adiabatic invariant, p the electron momentum, m_e its mass, and B the geomagnetic field strength) is nearly conserved by *both* pitch angle and radial diffusion operators [*Walt*, 1970], the spatiotemporal evolution of f can be approximately described by the following reduced diffusion equation [*Schulz and Lanzerotti*, 1974]:

$$\frac{\partial f}{\partial t} = L^{5/2}\frac{\partial}{\partial L}\left(\frac{D_{LL}}{L^{5/2}}\frac{\partial f}{\partial L}\right) - \frac{f}{\tau_L} \tag{1}$$

with $x = \cos\alpha_0$, $f = f(\zeta, x, L, t)$ and where both ζ and $y = \sin\alpha_0 = (1-x^2)^{1/2} \simeq 1$ are (nearly) conserved by radial diffusion and elastic pitch angle scattering. For the considered electrons with conserved $y \simeq 1$, one has $f(\zeta, x \sim 0, L, t) = f(M, J \sim 0, L, t)$ where J is the second adiabatic invariant, allowing us to use simply $f(M, L, t)$ in the following [*Schulz and Lanzerotti*, 1974]. Inward radial diffusion of such high pitch angle electrons should then lead to an increase of their momentum p roughly proportional to $1/L^{3/2}$ in a nearly dipolar geomagnetic field at $L < 4$.

To solve equation (1), we use approximate analytical expressions for D_{LL} and τ_L (see Appendixes A and B). In particular, we assume that radial diffusion from electrostatic perturbations clearly prevails in D_{LL} for $L \leq 4$, in agreement with several recent studies (see discussion in Appendix A and *Ozeke et al.* [2012]; *Tu et al.* [2012]; *Ozeke et al.* [2014]). As a result, one important condition used to derive the reduced equation (1) already turns out to be satisfied: D_{LL} is nearly independent of α above the loss cone edge (see equation (A1)). Next, we separate the full solution $f(L,t)$ into two parts F_L and F_α depending on D_{LL} and τ_L, respectively, and we derive approximate analytical solutions for each of these two parts (see Appendixes B and C).

Previous works have shown that although the average wave normal angle θ of hiss waves generally increases with geomagnetic latitude inside the plasmasphere, the lifetime τ_L of relativistic electrons is rather well approximated by assuming quasi-parallel waves with $\theta < 45°$[*Artemyev et al.*, 2013b; *Ni et al.*, 2013; *Glauert et al.*, 2014], allowing to recover measured lifetimes of 2–5 MeV electrons at $L \sim 2$–4 [*Meredith et al.*, 2009; *Agapitov et al.*, 2014; *Artemyev et al.*, 2013b; *Thorne et al.*, 2013a]. Consequently, we can use analytical estimates of τ_L obtained recently for quasi-parallel waves [*Mourenas and Ripoll*, 2012; *Mourenas et al.*, 2012b; *Artemyev et al.*, 2013b] and provided by equation (B1) in Appendix B. Moreover, we are looking here for an approximate solution to equation (1) for nearly equatorially mirroring electrons. The near conservation of $\zeta \equiv p^2L^3 \equiv M$ as these electrons are diffused radially inward finally leads to an approximate scaling $\tau_L(M,L) \sim E(M,L_0)^2(L_0/L)^{1.4}$ inside the plasmasphere at high energy $E > E_{\min} \sim 3.5(2/L)^{2.9}$ MeV (see Appendix B). As a result, the lifetime of such high-energy electrons turns out to be weakly dependent on L when considering (as below) inward diffusion over limited radial distances $\Delta L \leq 0.3L_0$ (with L_0 the initial location)—roughly fulfilling the second condition for the applicability of the reduced equation (1).

Since our main aim here is to provide very simple and practical analytical estimates, it is tempting to simplify our considerations on this basis—using a particular set of initial conditions. Namely, we shall assume that radial diffusion takes place from a preexisting narrow peak of energetic electron flux, allowing us to consider

a simplified formulation based on the *spatial broadening* within the plasmasphere of this narrow flux peak initially present at $L \simeq L_0$ (see Appendix C). Recent observations from the Van Allen Probes have demonstrated that such very localized *storage rings* of relativistic electrons, while rather uncommon, can indeed be created at $L_0 < 4$ during high geomagnetic activity periods [e.g., see *Baker et al.*, 2013; *Thorne et al.*, 2013b; *Baker et al.*, 2014]. We further assume that $\partial f/\partial L \sim 0$ at $L = L_0$ so that there is (almost) no inward or outward transport through the location $L = L_0$. In such a case, the spatial regions $L < L_0$ and $L > L_0$ are decoupled, and we can focus solely on the *inward* broadening (at $L \leq L_0$) of the flux peak. This situation may correspond, for instance, to a broadening of the flux peak occurring more or less symmetrically with respect to L_0—but it is not a necessary condition. In practice, the only requirement is that the gradient of $f(L)$ at $L \simeq L_0$ must remain much smaller than the very strong gradient present initially at $L < L_0$ in the vicinity of the peak. We shall see below that the initial presence of a not-too-narrow (i.e., realistic) flat maximum at $L \geq L_0$ in the actual flux distribution can be a favorable circumstance in this regard.

2.2. Approximate Analytical Solution for Inward Diffusion From a Preexisting Flux Peak at $L \sim L_0$

As inward radial diffusion is much faster near $L \sim L_0$ than at lower L, the particles spend ultimately much more time near their lowest L shell than near their initial location $\sim L_0$. Moreover, τ_L varies weakly with L. For the sake of simplicity, we can therefore use for τ_L in (1) its value $\tau_L(L)$ instead of some complicated average over the particle trajectory between L_0 and L. Accordingly, our full analytical estimate of $f(L, t)$ can be summarized as follows (see details in Appendixes A–C):

$$f(L,t) \sim \frac{1}{\sqrt{t}} \exp\left(-\frac{(L_0 - L)}{23.6 D_{LL}^0 L^5 t} - \frac{t}{\tau_L(M,L)}\right) \tag{2}$$

with τ_L from (B1), $f_m \sim 350$ Hz, $n_e = 3.5 \cdot 10^3 (2/L)^{3.1}$ cm^{-3} (inside the plasmasphere during moderately disturbed periods) [see *Meredith et al.*, 2007; *Agapitov et al.*, 2014; *Ozhogin et al.*, 2012], $B_w = 28(L/3.4)^{1/2}$ pT, and D_{LL} given by (A1). Equation (2) provides an approximate solution to equation (1) in the domain $0 < (L_0 - L) < 1.25, 2.5 \leq L_0 \leq 4, E > E_{\min} \sim 3.5(2/L)^{2.9}$ MeV and $t \geq t_{\min}$ with $t_{\min} = 0.003/(D_{LL}^0 L^5)$ (≈ 1 month for $K_p \sim 1.5$ and $L \sim 3$) where D_{LL}^0 is given in equation (A1).

To test the accuracy of our approximate analytical solution (2), we have performed comparisons with full numerical solutions to equation (1) obtained with the same lifetimes and D_{LL} values provided in Appendixes A and B. For the full numerical solution, we have used an implicit differential scheme and a tridiagonal matrix algorithm. One can see in Figure 1 that the approximate expression (2) remains rather close to the exact numerical solutions over the whole domain $0 < (L_0 - L) \leq 1$ between the initial time $t = t_0 = 1$ month $\geq t_{\min}$ and $t = 6$ months (for $L_0 = 3$ and $K_p = 3$ here).

It is worth emphasizing that the proposed analytical model should remain roughly accurate even if the initial electron distribution is not a narrow peak at $L = L_0$, but still possesses a steep slope there, as in the case of a step-like function. Actually, the main requirement for the approximations to hold is the presence of a strong gradient in the initial (at $t = t_0 \geq t_{\min}$) phase space density of relativistic electrons just below $L = L_0$, produced for instance by storm time energization. In the simplified analytical model, it is further assumed that the spatial broadening of the initial narrow flux peak also occurs at higher $L > L_0$, not necessarily symmetrically with respect to L_0 but in such a way that $\partial f/\partial L \sim 0$ at $L \sim L_0$ to have negligible inward/outward transport through $L = L_0$. In reality, electron transport through this location should remain weak due to both the reduced flux gradient close to the initial maximum and the important temporal decrease of the flux at larger $L > L_0$ caused by losses and a stronger radial transport toward the magnetopause [*Shprits et al.*, 2013; *Usanova et al.*, 2014; *Ma et al.*, 2015; *Turner et al.*, 2012; *Ukhorskiy et al.*, 2015] (e.g., see solid curves in Figure 1). At sufficiently low $L \leq L_0 - 0.2$, the electron distribution should then depend weakly on the exact shape of the initial distribution at $L > L_0$, as confirmed by numerical simulations displayed in Figure 1 for different spatial widths of the initial phase space density (PSD) profile at $t = t_0 = 1$ month. Nonetheless, a slightly wider initial maximum in the actual flux leads to a better agreement with analytical estimates very close to L_0 at later times, because a wider and flatter initial distribution at $L > L_0$ leads to a weaker negative slope of $f(L)$ near $L \sim L_0$.

While this new approximate model of radial diffusion coupled with pitch angle diffusion is not the first analytical model of its kind, nor probably the most accurate one, it does provide much more simple and practical estimates than the more comprehensive models developed in the past [*Chiu et al.*, 1988; *Schulz and Newman*, 1988]—although it should be used only for specific but realistic initial conditions corresponding to satellite observations of a flux peak at low L.

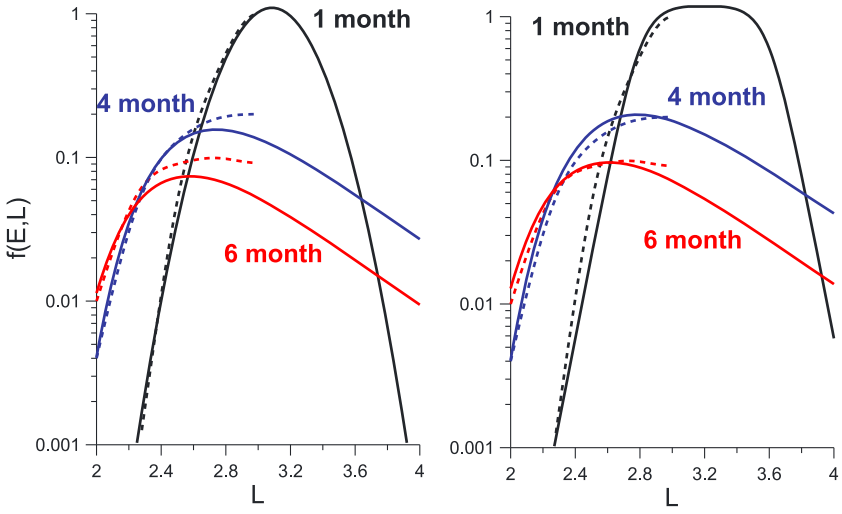

Figure 1. Spatiotemporal evolution of the relativistic electron PSD for different sets of initial conditions. The black dashed curves show the initial PSD profile at $L \leq L_0 = 3$ obtained with the simplified analytic model (2) at $t = t_0 = 1$ month $\geq t_{min}$. Solid black curves show more realistic types of initial distributions used in full numerical simulations solving equation (1), with either (left) a very narrow flux peak or (right) a sensibly wider maximum at t_0. We consider electrons with $M = 3800$ MeV/G, and the PSD profiles are shown for $K_p = 3$ at the initial time $t_0 = 1$ month, as well as at $t = 4$ and 6 months (blue and red curves, respectively) as obtained from full numerical simulations (solid curves) and analytical estimates (dashed curves).

3. Comparisons With Observations

To test the applicability of the approximate formulation (2) in a real situation, the analytical electron PSD has been compared with measurements obtained on board the Van Allen Probes at $L \sim 2.5-3.5$ after the creation of a narrow peak of relativistic electron flux at $L_0 \simeq 3.5-4$ in early October 2012. This peak was probably produced by chorus-induced energization of initially 100–300 keV electrons at $L \sim 3.5-4.5$ during the early recovery phase of a particular storm [*Baker et al.*, 2013; *Thorne et al.*, 2013b; *Baker et al.*, 2014; *Mourenas et al.*, 2015, 2012a] followed by losses to the atmosphere induced by chorus or electromagnetic ion cyclotron (EMIC) waves at $L > 4$ [*Shprits et al.*, 2013; *Usanova et al.*, 2014] and subsequent outward radial diffusion at higher L [*Turner et al.*, 2012].

The electron distribution function $f(E)$ is related to the differential flux $j(E)$ by $f(E) = j(E)/p^2 \sim j(E)/E^2$ for $E > 1$ MeV [*Schulz and Lanzerotti*, 1974], allowing to switch from phase space density to differential flux. The differential flux can be written as $j(E(M,L)) \sim f(E(M,L))K_0(E(M,L_0))$, where K_0 provides the normalization of the differential flux $j \sim E^2 f$ based on the initial flux level as well as its initial spectral shape, i.e., its variation with E at $L = L_0$. Generally, one can use an approximate kappa (or generalized Lorentzian) distribution $K_0 \sim E(M,L)^{-\kappa}(L_0/L)^{3\kappa/2}$ where κ typically varies between 2 and 12 [e.g., see *Xiao et al.*, 2008; *Livadiotis*, 2015]. For instance, the storm period from 12 UT to 24 UT on 17 March 2013 corresponds to $\kappa \approx 4$ to 10 for $E \geq 3$ MeV at $L \sim 3.5$ [*Li et al.*, 2014a; *Mourenas et al.*, 2015]. Let us consider more specifically the period between October 2012 and February 2013 at $L = 2.5-3.5$. A comparison of the differential flux levels at various energies measured by the Van Allen Probes on 2 November 2012 shortly after the formation of a peak of flux at $L_0 \sim 3.5$ (see Figure 3 from *Baker et al.* [2014]) shows that $\kappa \approx 7.5$ in this case. Using $K_p \approx 1.5$ as a rough mean value between October 2012 and February 2013, we also deduce an average magnitude of the radial diffusion rate $D^0_{LL} \approx 5 \cdot 10^{-7}$ day^{-1} during the same period.

Figure 2 shows a comparison between the analytical differential flux $j(E, L, t)$ and actual measurements from the Van Allen Probes between November 2012 and February 2013 [*Baker et al.*, 2014], normalized to the flux value at $L_0 = 3.5$ and $t_0 \sim 1$ month (after the production of the initial flux peak). Note that the latter values of L_0 and t_0 allow fitting the observed fluxes at $t \sim t_0 \sim 1$ month, therefore providing pretty good initial conditions for the analytical model. From that time onward, the general spatiotemporal behavior of the measured flux (i.e., its inward diffusion and decrease) is roughly recovered by the approximate analytical model for both $E = 7.2$ MeV and $E = 3.6$ MeV, demonstrating the overall reliability of our basic assumption that inward radial diffusion can be approximately described as the spatial broadening of a preexisting flux peak in this case.

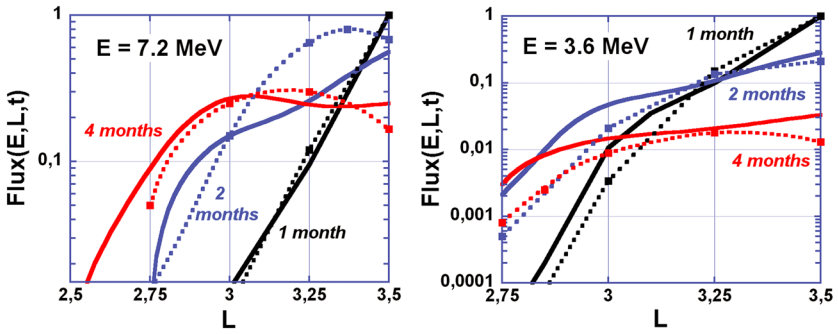

Figure 2. Spatiotemporal evolution of the differential electron flux $j(E, L, t)$ for $E = 3.6$ MeV and $E = 7.2$ MeV at $L = 2.5–3.5$, for $t = 1$ month, 2 months, and 4 months (black, blue, and red curves, respectively) after the 9 October 2012 strong production of relativistic electrons at $L_0 \sim 3.5$. The analytical results are displayed by solid curves, while the corresponding measurements from the Van Allen Probes [*Baker et al.*, 2014] are shown by dotted curves with square symbols. The value of j is normalized to its level in $L_0 = 3.5$ at $t_0 \simeq 1$ month.

The main discrepancy between analytical and measured fluxes is the presence, around 2 months after the start, of a small bump of measured flux at $L \sim 3.25$ very close to L_0. This feature is not recovered by the approximate model. It might stem in part from the presence at earlier times of a wider, not fully flat maximum (going from $L \sim 3.5$ to 3.8) in measured fluxes [*Baker et al.*, 2014] than in the simplified model, which relies on the assumption of a narrow peak at $L \sim L_0 = 3.5$. A wider initial maximum with a slight bump above L_0 could produce an additional arrival of electrons at $L \sim L_0 - 0.5$ to $\sim L_0$ before being smoothed out at later times. The slightly lower flux levels in measurements at $L \sim 2.5–3$ could easily be explained by a $\sim 25\%$ reduction of either the lifetime τ_L or the radial diffusion rate D^0_{LL} of relativistic electrons or by a combination of smaller decreases of both. For instance, a 25% reduction of the plasma density as compared with its average value given by *Ozhogin et al.* [2012] would be enough to reduce τ_L to an adequate level. Such decreases are well within the statistical range of variation (a factor ~ 3) of τ_L and D_{LL} around their mean value [*Sicard-Piet et al.*, 2014; *Ozeke et al.*, 2014] while remaining also within the uncertainty range of our analytical estimates (a factor ~ 1.5).

The flux of relativistic electrons managing to reach $L \sim 2.5$ remains negligible in this case, smaller than 1% of the maximum flux measured nearly 1 month after the formation of the initial flux peak at $L_0 \sim 3.5$. These results are consistent with many other observations. Relativistic electron injections into the slot and inner belt are relatively rare [*Zhao and Li*, 2013a; *Li et al.*, 2015; *Fennell et al.*, 2015] and occur mainly during extremely strong interplanetary shocks [*Blake et al.*, 1992; *Li et al.*, 1993] and geomagnetic storms [*Baker et al.*, 2004].

4. Potential Uses of the Simplified Analytical Model

4.1. Determination of (L, E, t) Regions Corresponding to a Prevalence of Radial Diffusion or Atmospheric Losses

As when considering energy diffusion in the presence of atmospheric losses [*Mourenas et al.*, 2014], there are two possible regimes for the considered spatial broadening of the electron distribution: a loss-limited regime of radial diffusion corresponding to losses faster than inward diffusion and a regime of negligible losses over the typical time scale of radial transport for large enough lifetimes τ_L and/or radial diffusion rate D_{LL}. Let us examine these regimes in more details.

At any particular location $L < L_0$ and for any given electron energy E, the electron PSD $f(L, t)$ described by equation (2) first increases quickly with time, then reaches a maximum at a time t_{max} given by

$$t_{max} \approx \frac{\tau_L}{2}\left(-\frac{1}{2} + \sqrt{\frac{1}{4} + \frac{4(L_0 - L)}{AD^0_{LL}L^5\tau_L}}\right). \quad (3)$$

and later on decays exponentially with a characteristic time scale $\sim \tau_L$. Here as well as in the remainder of this paper, one can take $A = 23.6$ as given by equation (C3). Accordingly, inward radial diffusion at any particular L mainly takes place when $t \leq t_{max}(E, L)$ before the increased electron fluxes get progressively washed out at $t > t_{max}$. The existence of a loss-limited regime of radial diffusion therefore requires that the characteristic time scale for radial transport $\approx t_{max}$ be larger than $\sim \tau_L/3$ so that atmospheric losses can effectively limit

radial diffusion. It corresponds to a condition $AD_{LL}^0 L^5 \tau_L/(L_0 - L) < 4$. Making use of the approximate expression for $\tau_L(M, L)$ inside the plasmasphere given by equation (B1) for fixed invariant M, this condition can be rewritten as

$$E(L) < E_{\text{max,loss-limited}}(\text{MeV}) \sim \frac{3.2\sqrt{L_0 - L}}{L^{3.3}\sqrt{AD_{LL}^0}}, \tag{4}$$

showing that efficient pitch angle scattering loss of highly relativistic electrons occurs mainly at lower L shells. In this loss-limited regime of radial diffusion, one gets

$$t_{\text{max}}(\text{day}) \sim \frac{\sqrt{(L_0 - L)\tau_L}}{\sqrt{AD_{LL}^0 L^5}} \approx \frac{E(\text{MeV})\sqrt{L_0 - L}}{2L^{3.2}\sqrt{D_{LL}^0}} \tag{5}$$

corresponding typically to $t_{\text{max}} \sim 1$–6 months for $E \sim 2$–6 MeV, $L \sim 2$–3, and $K_p \sim 1.5$. Conversely, electrons of high enough energy $E > E_{\text{max,loss-limited}}$ are diffused radially inward in a nearly lossless regime. It is also worth noting that over a substantial laps of time $0.7t_{\text{max}} \leq t \leq 2t_{\text{max}}$, losses to the atmosphere are roughly balanced by inward transport of electrons, leading to a very slow local decrease of trapped fluxes. *Apparent* lifetimes deduced from satellite measurements during this period will appear much longer than the actual τ_L due to pitch angle scattering alone. The presence of inward diffusion from a flux maximum at $L \geq 3.5$ could therefore explain some very long decay time scales of relativistic electrons recently measured at $L \sim 3.1$–3.3 by the Van Allen Probes [*Ni et al.*, 2015].

Step-by-step details on how to use the proposed method in practice to determine domains of prevalent radial diffusion or losses are provided in Appendix D.

4.2. Conditions for Relativistic Electron Access to the Inner Belt

The logical next step is to examine what kinds of conditions could actually allow the access of relativistic electrons to the Earth's innermost radiation belt at $L < 2$. This issue is of high interest for estimating the average relativistic electron content of the inner belt over the long term. Of course, as discussed further below, an extremely strong storm (or interplanetary shock) injecting directly such electrons at $L \sim 2 - 2.5$ would certainly succeed. But the key question that we would like to answer is whether the more frequent formation of an initial maximum of relativistic electron flux at $L_0 \approx 3$ could also achieve that goal under certain—as yet unspecified—circumstances.

Based on the proposed model of inward diffusion from a preexisting flux peak, let us assume that a finite level of electron PSD reaches $L < L_0$ at a time $t > t_0$ so that $f(M, L, t) \sim f(M, L_0, t_0)/\Delta$, with $\Delta \gg 1$ the reduction of the PSD level between (L_0, t_0) and (L, t). For t typically comprised between $\sim 2t_0$ and $\sim 7t_0$, the latter equation can be rewritten as $L(L_0 - L)/(AD_{LL}^0 L^6 t) + t/\tau_L \simeq \ln(\Delta\sqrt{t_0/t}) + (t_0/\tau_L)(L_0/L)^{1.4}$. Neglecting to first order the weak variation with t of the first term on the right-hand side, it yields a second order equation in t, which has a real solution (i.e., positive discriminant) only for

$$AD_{LL}^0 L^6 \tau_L \geq \frac{4L(L_0 - L)}{\left(\ln(\Delta/2) + (t_0/\tau_L)(L_0/L)^{1.4}\right)^2}. \tag{6}$$

For large enough electron energy E and/or PSD reduction Δ such that $\tau_L(M, L) \gg t_0(L_0/L)^{1.4}/\ln(\Delta/2)$, one can further deduce from equation (6) a rough estimate of the maximum inward radial diffusion $(L_0 - L)_{\text{max}}$ of energetic electrons such that $f(M, L, t) \sim f(M, L_0, t_0)/\Delta$, giving finally

$$\frac{(L_0 - L)_{\text{max}}}{L} \sim \frac{AD_{LL}^0 L^4 \tau_L(M, L)\ln^2(\Delta/2)}{4} \approx \left(\frac{E_{L=3}}{7\text{MeV}}\right)^2 \left(\frac{L}{3}\right)^{2.6} 10^{-2.3+0.46K_p} \ln^2(\Delta/2) \tag{7}$$

where the corresponding minimum L should be reached at $t \sim \tau_L(M, L)\ln(\Delta/2)/2 \leq t_{\text{max}}$. Equation (7) shows that inward radial diffusion is more limited at $E \sim 1$–2 MeV than at higher energy (due to the larger lifetimes of higher-energy electrons inside the plasmasphere). It is also more constrained at lower L (due to weaker radial diffusion).

Using typical plasmaspheric parameters from (2) and $E = 7.2$ MeV for $L_0 = 3.5$ and $t_0 = 1$ month, even a relatively low level of PSD (e.g., $f(L = 3, t) \sim f(L_0, t_0)/20$) can only be attained after at least $\sim$ 4 months

of continuous radial diffusion with $K_p = 1.5$. The above estimates clearly demonstrate that inward radial diffusion of relativistic electrons should generally be confined to the vicinity of the initial flux peak within the plasmasphere—hiss-induced losses effectively preventing such electrons initially injected at $L_0 > 3$ from diffusing down to the inner radiation belt. However, one can also notice from equation (7) that prolonged periods of dramatically enhanced radial diffusion corresponding to $K_p > 5$ may still allow highly relativistic electrons to travel inward quite far. It would correspond to a lossless regime of very strong radial diffusion, for which the characteristic time scale for reaching L becomes $t_{srd} \approx t_{\max}/4 \sim (L_0 - L)/(2AL^5 D_{LL}^0)$ (~ 1 week typically).

The peak of relativistic electron flux brought about by strong storms occurs generally around $L_{\max} \sim 1.2\ L_{pp}$ [*O'Brien et al.*, 2003; *Li et al.*, 2006] just above the plasmapause location L_{pp} [*O'Brien and Moldwin*, 2003]. Accordingly, the situation $L_0 > 3$ corresponds to most geomagnetic storms such that $K_p < 7.5$ or $D_{st} > -200$ nT. The intrusion of relativistic electrons at $L < 2$ requires either an extreme geomagnetic storm, or a strong storm with a prolonged recovery phase of high $K_p > 5$, or else a protracted period (months) of relatively moderate K_p with reduced hiss wave intensity. On the other hand, it is worth noting that *extremely relativistic* electrons such that $E(L_0) > E_{\text{max,loss-limited}}(L/L_0)^{3/2}$, once hypothetically produced at $L_0 \leq 3$, could easily be diffused inward to $L < 2$ in a loss-free regime, owing to their much longer lifetimes. When considering relativistic particles, therefore, only such very high energy electrons (with $E > 20$ MeV for a mean $K_p < 3$) should be able to reach the inner belt in general. Although such events are probably rare, it is worth noting that injections of electrons of tens of MeV at $L \sim 2-3$ have been observed after the March 1991 strong interplanetary shock [*Blake et al.*, 1992; *Looper et al.*, 2005] as well as after the October 2003 strong geomagnetic disturbance during which D_{st} reached −400 nT [*Looper et al.*, 2005].

However, very low energy electrons with $E < 200$ keV have very long lifetimes as well, due to their lack of cyclotron resonance with hiss and lightning-generated waves at low L (see estimates and simulations in *Artemyev et al.* [2013b] and *Agapitov et al.* [2014]). As a result, they may also be easily diffused inward down to the inner belt. Such low-energy electrons will, however, gain energy while being diffused inward, due to the conservation of the first adiabatic invariant M. Thus, such a (rough) upper limit $E < 200$ keV at their initial location $L_0 \geq 2.5$ will eventually translate into higher upper limits on the energy of incoming fluxes $E < 350$ keV at $L = 2$ and $E < 700$ keV at $L = 1.5$. This is roughly consistent with recent observations [*Zhao and Li*, 2013b; *Zhao et al.*, 2014, 2015] that electron injections at $E < 600$ keV in the slot and inner belt occur rather frequently (several times per year), with pitch angle and spatial distributions showing unambiguously that such recorded electron populations are real and not produced by proton contamination in the sensors [*Zhao et al.*, 2014; *Li et al.*, 2015; *Fennell et al.*, 2015].

Let us consider in more details below some of the possible scenari for relativistic electron access to the inner belt. Actually, a combination of hiss mean frequencies ω_m slightly higher than usual, coupled with an elevated radial diffusion rate corresponding to $K_p \simeq 3$ (or to the upper quartile of ULF wave measurements for $K_p = 2$) [*Ozeke et al.*, 2014] might also allow $E > 5$ MeV electrons to diffuse radially inward from $L_0 \sim 3$ down to the inner belt during moderately disturbed conditions, because relativistic electron lifetimes increase roughly like $\sim \omega_m^{7/9}$ [*Mourenas et al.*, 2012b; *Artemyev et al.*, 2013b]. The mean frequency of plasmaspheric hiss might get increased for an extended period if, for instance, chorus waves are initially generated near one tenth of the local electron gyrofrequency just outside of a slightly closer plasmapause, before propagating into the plasmasphere to form an embryonic source for hiss waves [*Bortnik et al.*, 2011; *Chen et al.*, 2012]. This is roughly consistent with CRRES statistics at $L = 2-2.5$ showing that the frequency of peak hiss intensity rises during more disturbed conditions [*Meredith et al.*, 2007].

Accordingly, we have considered a situation such that the mean frequency of hiss waves is near 650 Hz and $D_{LL}^0 \sim 2.5 \cdot 10^{-6}$ day^{-1}, with an initial peak of relativistic electron PSD at $L_0 = 3$. The corresponding analytical PSD $f(M, L, t)$ is displayed in Figure 3 (left), as well as for a more usual mean hiss frequency of 350 Hz and $D_{LL}^0 \sim 5 \cdot 10^{-7}$ day^{-1} as before. Figure 3 shows that when using average wave and plasma parameters for $K_p \leq 1.5$, relativistic (5.5 MeV) electrons coming from $L_0 = 3$ are unable to reach $L < 2.55$—even after more than 6 months. In contrast, using a slightly higher hiss frequency and an enhanced radial diffusion coefficient corresponding to the upper quartile of ULF wave measurements for $K_p = 2$, the level of $f(M, L)$ at $L \simeq 2$ could reach after 5–6 months about 2% of its maximum value at $L = L_0 = 3$. Using the same hiss frequency as

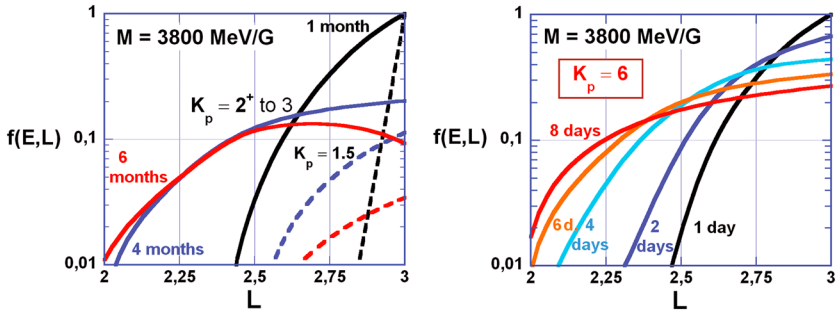

Figure 3. (left) Spatiotemporal evolution of the analytical electron PSD $f(M, L, t)$ obtained for $M = 3800$ MeV/G at $L = 2–3$ between 1 and 6 months after a strong burst of relativistic electrons at $L_0 \sim 3$. The value of f is normalized to its level in $L_0 = 3$ at $t_0 = 1$ month. The phase space density $f(L, t)$ is calculated for $K_p = 3$ (or the upper quartile of $K_p = 2$) and a mean hiss frequency of 650 Hz (solid lines) as well as for $K_p \sim 1.5$ and a smaller mean frequency (350 Hz) of plasmaspheric hiss waves (dashed lines). (right) Spatiotemporal evolution of the analytical electron distribution $f(M, L, t)$ obtained for $M = 3800$ MeV/G at $L = 2–3$ between 1 and 8 days after a strong burst of relativistic electrons at $L_0 \sim 3$. The value of f is normalized to its level in $L_0 = 3$ at $t_0 = 1$ day. The phase space density $f(L, t)$ is calculated for $K_p = 6$, corresponding to a prolonged substorm activity during the recovery phase of a strong storm, with twice smaller lifetimes than during moderately disturbed periods.

before, this level at $L \sim 2$ would be reduced by a factor ~ 1.5 for $t = 6$ months. It definitely shows that the actual magnitude of D_{LL} is the most important factor for a deep penetration of relativistic electrons.

Other favorable conditions correspond to strongly disturbed periods—for example, a prolonged period of substorms with $K_p \sim 5–6$ during the recovery phase of a strong storm assumed to have produced a peak of flux just above $L_0 = 3$. Replacing in equation (6) the quiet time electron lifetime τ_L by an approximate lifetime $\sim \tau_L/2$ corresponding to twice higher hiss intensity during such periods [*Meredith et al.*, 2009; *Agapitov et al.*, 2014], one finds that D^0_{LL} must be larger than $(L_0 - L)/(35\tau_L L^5)$ to get $f(L = 2, t)/f(L_0 = 3, t_0 = 1 \text{ day}) > 1/40$ after 1 week. Figure 3 (right) shows the evolution of the phase space density for $M = 3800$ MeV/G obtained for a strong radial diffusion $D^0_{LL} = 5.75 \cdot 10^{-5}$ day^{-1} satisfying the latter condition, between 1 and 8 days after an important burst of relativistic electrons at $L_0 \sim 3$. The considered relativistic electrons manage to reach $L = 2$ after 6 days of sharply enhanced radial diffusion. The smaller lifetimes have almost no effect in this lossless regime of very strong radial diffusion. Actually, this kind of situation could more or less correspond to two important storms of August–September and November 1998 during which geomagnetic activity remained elevated for ~ 4 days, apparently accompanied by a progressive inward diffusion of 2–6 MeV electrons from $L \sim 3$ down to $L \sim 2.2$ recorded by Solar Anomalous and Magnetospheric Particle Explorer [*Li et al.*, 2001].

Finally, the evolution of the differential flux $j(E, L, t)$ has been plotted in Figure 4 in the case of a long period of enhanced radial diffusion corresponding to $K_p = 3$ or the upper quartile of $K_p = 2$ (this time with usual, average lifetimes). We have further assumed an initial energy variation $j(E, t = 0) \sim 1/E^\kappa$ with $\kappa = 7.5$ between ~ 50 keV and 7.5 MeV, corresponding to an earlier heating of the electron distribution by intense chorus waves at $L \geq L_0 = 3$ [*Mourenas et al.*, 2015].

The inward radial diffusion of low-energy electrons (with $E \sim 150$ keV, thus assumed to have infinite lifetimes) [see *Artemyev et al.*, 2013b] occurs in a lossless regime, allowing them to reach the inner belt in large numbers after about 3 months. In sharp contrast, fluxes of relativistic electrons with $E = 3.5$ MeV remain confined at $L > 2.25$ over the whole 6 months period, decreasing rapidly with time due to their relatively short lifetimes $\tau_L < 30$ days. Electrons belonging to the intermediate energy range $E \sim 0.5–2$ MeV remain similarly confined close to $L = L_0$ (not shown). As the energy of relativistic electrons increases from 3.5 MeV to 7.5 MeV, a progressive extension of the domain of strong fluxes toward lower L shells can be noticed. The inward diffusion of electrons such that $E \sim 1–15$ MeV $< E_{\text{max,loss-limited}}$ proceeds in a loss-limited regime. Nevertheless, fluxes of 7.5 MeV electrons already come quite close to the behavior expected in a lossless regime of radial diffusion (e.g., compare with fluxes at 150 keV in Figure 4). This interesting feature actually stems from the strong energy variation of the initial distribution: particles reaching $L = 2$ have been accelerated all along their way from $L_0 \sim 3$ and therefore correspond to a much higher level of initial flux $j(E, L_0, t = 0)$ at lower energies.

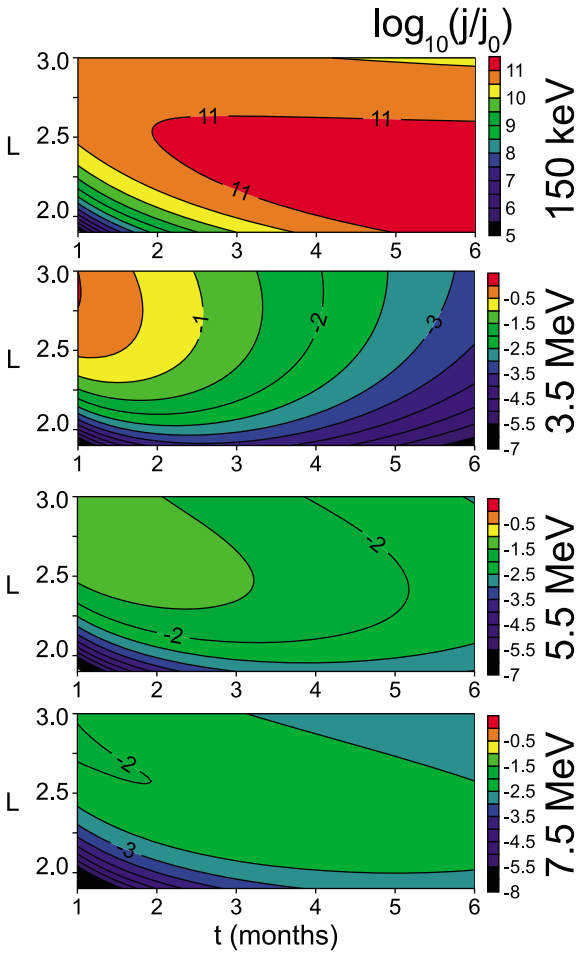

Figure 4. Maps of the spatiotemporal evolution of the analytical differential electron flux $j(E, L, t)$ over $L = 1.9–3$ between 1 and 6 months after a strong burst of relativistic electrons at $L_0 = 3$. The value of j is normalized to its level j_0 in $L_0 = 3$ at $t_0 = 1$ month for $E = 3.5$ MeV. An elevated value of D_{LL}^0 corresponding to $K_p \simeq 3$ (or to the upper quartile of $K_p = 2$) is used together with usual average lifetimes and an approximate $\kappa = 7.5$ for the initial distribution. Various electron energies are considered.

Although this effect partly compensates losses to the atmosphere, it would quickly disappear for smoother initial energy distributions (i.e., for smaller values of κ).

While highly relativistic electrons might therefore be able to attain the inner belt under very favorable circumstances, a statistical analysis of the corresponding required wave and plasma conditions over one or more solar cycles would be necessary to assess the probability of such events.

4.3. A Simple Means for Inferring Average Radial Diffusion Rates Within the Plasmasphere

The approximate analytical solutions could also be used to infer the magnitude of the average radial diffusion rate D_{LL} from a careful analysis of the measured distribution of nearly equatorially mirroring relativistic electrons during appropriate circumstances, corresponding to a preexisting flux peak of relativistic electrons at $L \sim L_0 < 4$ inside the plasmasphere. Detailed instructions for using the proposed method in practice are given in Appendix D. Similar but more comprehensive and complicated methods have been proposed previously [e.g., see *Tomassian et al.*, 1972; *Chiu et al.*, 1988]. To mitigate the errors that may arise from a comparison of different energy channels of particle counters, one can further consider the electron distribution measured at two different times at the same energy. Making use of equations (A1)–(B1), the ratio of electron PSD $f(M, L, t)$ obtained at two times t_1 and $t_2 > t_1$ after the start of inward radial diffusion from L_0 can be written as

$$\frac{f(t_2)}{f(t_1)} = \frac{t_1^{1/2}}{t_2^{1/2}} \exp\left(\frac{(t_2 - t_1)(L_0 - L)}{A t_1 t_2 D_{LL}^0 L^5} - \frac{(t_2 - t_1)}{\tau_L} \right) \tag{8}$$

at fixed location $L < L_0$ and first adiabatic invariant M (or energy E). An expression giving $D_{LL}^0 = D_{LL}(L = 1)$ as a function of the ratio of the distribution levels can be readily derived from equation (8):

$$D_{LL}^0\ (\text{day}^{-1}) = \frac{(t_2 - t_1)(L_0 - L)/(A t_1 t_2 L^5)}{\ln\left(\frac{t_2^{1/2} f(t_2)}{t_1^{1/2} f(t_1)} \right) + \frac{(t_2 - t_1)}{\tau_L}} \tag{9}$$

where times t_1, t_2, and τ_L are in units of days.

Based on the above expression (9), the inferred value of D_{LL}^0 should be more reliable when the ratio $t_2^{1/2} f(t_2)/(t_1^{1/2} f(t_1))$ is larger than the term $(t_2 - t_1)/\tau_L$, which depends on different parameters such as hiss wave frequency and amplitude as well as plasma density, which may all vary significantly with time. Thus, the best conditions correspond to high relativistic electron energy at relatively low L shells, a relatively high ratio $t_2/t_1 \sim 2 - 4$, at a distance $(L_0 - L) \geq 0.5$ from the initial flux maximum. In addition, the proposed method postulates the prevalence of hiss waves in determining relativistic electron losses to the atmosphere. Consequently, a small enough level of EMIC waves is further required at $L < 3.5$ deep inside the plasmasphere, as it is usually the case during moderate geomagnetic activity with $K_p < 2$ [*Meredith et al.*, 2014; *Wang et al.*, 2014].

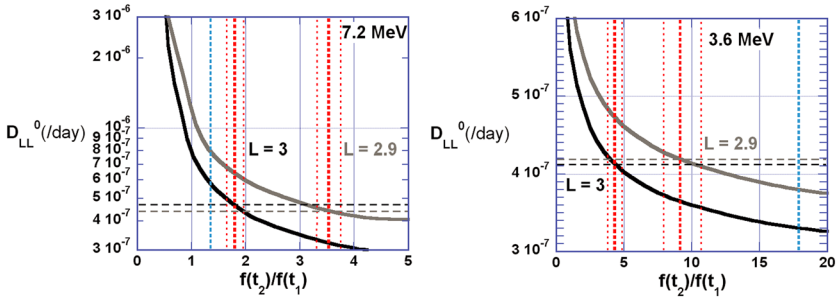

Figure 5. Radial diffusion coefficient $D_{LL}^0 = D_{LL}(L = 1)$ obtained from equation (9) as a function of the ratio $f(E, L, t_2)/f(E, L, t_1)$ of the phase space density of relativistic electrons obtained at two different times after their initial acceleration on 9 October 2012 slightly above $L_0 = 3.5$. We consider $L = 3$ (solid black line) and $L = 2.9$ (solid grey line). The vertical blue dotted line indicates the abscissa for which the term including the ratio $f(t_2)/f(t_1)$ is equal to the (loss) term proportional to $1/\tau_L$ at the denominator of equation (9). The large red dotted line shows the value of $f(t_2)/f(t_1)$ obtained from the Van Allen Probes [*Baker et al.*, 2014] with an uncertainty showed by thin dotted red lines. The horizontal black (grey) dashed line shows the corresponding level of D_{LL}^0 given by the intersection of the large dotted red and solid black (grey) lines. The results for electrons of energy (left) $E = 7.2$ MeV (t_1 and t_2 corresponding to 3 December 2012 and 3 February 2013) and (right) 3.6 MeV (t_1 and t_2 corresponding to 2 November 2012 and 3 February 2013).

Figure 5 shows the radial diffusion rate D_{LL}^0 inferred with the help of equation (9) from Van Allen Probes measurements [*Baker et al.*, 2014] of relativistic electron fluxes at two different times at $L = 3$ and 2.9 after the production on 9 October 2012 of an initial peak near $L_0 = 3.5$. The results for both the 7.2 MeV and 3.6 MeV electrons are very similar, giving $D_{LL}^0 \sim 4.15 \cdot 10^{-7}$ day^{-1} and $D_{LL}^0 \sim 4.55 \cdot 10^{-7}$ day^{-1}, respectively. Such levels of radial diffusion look rather realistic, since they correspond to D_{LL} levels predicted by *Ozeke et al.* [2014] for a value of $K_p \simeq 1.38$ close to the average level of geomagnetic activity during that period.

The inferred D_{LL}^0 depends also on the chosen value of L_0 which, as discussed in section 2.5, should correspond to the start of a steep fall of flux toward lower L a few weeks after the production of the initial peak of relativistic electron flux by chorus wave energization. In the considered test case [*Baker et al.*, 2014], this value of L_0 could be varied between ~ 3.4 and ~ 3.7. Using equation (9), it corresponds to an uncertainty of about 30% on the inferred D_{LL}^0 as compared with its mean value, which remains quite reasonable.

The above results look promising for a possible determination of radial diffusion rates on the basis of relativistic electron flux measurements after the storm time production of an initial peak at $L_0 < 4$ inside the plasmasphere. The uncertainty related to electron lifetime estimates can really be strongly reduced by comparing relativistic electron fluxes at high enough energy. But we hasten to add that very favorable circumstances are needed, such as a steep gradient in phase space density near the location of the initial burst of relativistic electron flux, a fast refilling of the plasmasphere, and an extended period of moderate geomagnetic activity afterwards (as well as a near absence of EMIC waves in the region $L < L_0$). Thus, one can expect that such conditions should be satisfied only once or twice per year. A careful statistical study would be needed to assess the actual reliability of this method, but it is left for future works.

5. Conclusions

In this paper, we have considered specific circumstances such that radial diffusion from a preexisting flux peak and losses to the atmosphere via pitch angle scattering by hiss waves are the prevalent processes determining the fate of relativistic electrons inside the plasmasphere. Such a particular set of initial conditions actually corresponds to some (relatively rare) observations of storage rings of relativistic electrons encircling the Earth at $L_0 \sim 3$–3.5 [*Baker et al.*, 2013]. It has allowed us to provide an approximate but very convenient analytical description of the spatiotemporal evolution of the trapped electron distribution. The analytical phase space density has been compared with observations on board the Van Allen Probes, showing a reasonable agreement during an extended period of moderate geomagnetic activity in the aftermath of one important storm.

While the proposed simplified analytical estimates cannot replace precise full-scale three-dimensional numerical simulations, they could help in the future to quickly analyze and better understand the dynamics of the

trapped electron fluxes in both numerical simulations and satellite observations, by determining the relative importance of each individual process via an easy parametric study of the flux variations.

Moreover, the conditions allowing the access of relativistic electrons to the inner belt ($L < 2$) can been roughly determined on this basis, as a function of various parameters. It has been shown that, apart from an injection occurring already at $L < 2.5$, some favorable conditions might allow relativistic electrons (>1 MeV) to travel from $L \sim 3$ to $L \sim 2$. It can correspond either to a higher hiss frequency coupled with slightly enhanced radial diffusion over about 5 months or else one full week of strongly enhanced radial diffusion with $K_p \sim 5 - 6$. But during most circumstances, it is found that relativistic electrons should remain confined to the domain $L > 2.7$, which agrees well with recent measurements and statistics [*Baker et al.*, 2014; *Fennell et al.*, 2015; *Li et al.*, 2015]. More comparisons with satellite measurements are planned in the future.

The very low likelihood of events potentially leading to direct injection or radial diffusion of relativistic electrons into the inner belt supports the conjecture of *Kim and Shprits* [2012] that any negative gradient in the phase space density of ≈ 0.5–1 MeV electrons toward higher L in the region $L \sim 1.5–2$ [e.g., see *Abel et al.*, 1997; *Kim and Shprits*, 2012; *Fennell et al.*, 2015] would result either from very rare intrusions followed by very long periods (∼ year) dominated by losses to the atmosphere stronger at higher L in this region [*Agapitov et al.*, 2014] or from a local acceleration of lower energy (∼ 100 keV) electrons via resonant scattering by lightning-generated and VLF waves peaking near $L = 1.5 - 1.7$. However, energy diffusion by whistler-mode waves would require years to produce such a flux maximum [*Agapitov et al.*, 2014].

Finally, it has been shown that, under appropriate circumstances, the proposed analytical model could be used to infer the magnitude of radial diffusion rates directly from measurements of ultrarelativistic electron fluxes at various times during long periods of moderate disturbances, following the production of a large initial peak of flux at low $L < 4$. Accurately quantifying radial diffusion rates is critically important for allowing radiation belt codes to reproduce and forecast the variability of relativistic electron flux observed by satellites. Therefore, new evaluations based on in situ electron flux measurements might complement the existing radial diffusion rates obtained from ground-based ULF wave measurements [*Ozeke et al.*, 2014]. While more work is still needed to better assess the reliability of the proposed method, previous and more precise similar methods [*Tomassian et al.*, 1972; *Chiu et al.*, 1988] can also benefit from the provided estimates of the parameter ranges corresponding a priori to a better accuracy.

Appendix A: Approximate Radial Diffusion Coefficients at $L \sim 2–4$

As concerns radial diffusion driven by ULF fluctuations, a number of models have been developed since the pioneering works of *Falthammar* [1965] and [*Schulz and Lanzerotti*, 1974]. Most notably, *Brautigam and Albert* [2000] have provided separate electrostatic and electromagnetic radial diffusion coefficients which have been used extensively ever since in radiation belt codes [*Shprits and Thorne*, 2004; *Su et al.*, 2010; *Turner et al.*, 2012; *Glauert et al.*, 2014; *Tu et al.*, 2014]. Their electrostatic diffusion coefficient was derived by assuming that the electric field spectrum corresponds to a convection electric field with a rapid rise and an exponential decay, while their electromagnetic diffusion coefficient was based on compressional magnetic field measurements. In particular, they showed that D_{LL}^{ES} varied roughly like L^6, while $D_{LL}^{EM} \sim L^{10}$. However, they had to rely on the limited number of measurements available at that time as well as some auxiliary assumptions.

Building on more recent strings of measurements (ULF electric field power mapped from ground magnetometer data and compressional magnetic field power from in situ measurements) as well as on results from new magnetohydrodynamic codes, *Ozeke et al.* [2012, 2014] and *Tu et al.* [2012] have concluded that the magnetic diffusion term can generally be neglected as compared with the electric field term. Numerical simulations of radial diffusion of electrons at $L = 2 - 3$ have also indicated a probable variation $D_{LL} \sim L^6$ there [*Zhao and Li*, 2013b]. *Ozeke et al.* [2014] have provided new analytical expressions of this dominant electric field radial diffusion coefficient based on 15 years statistics of ULF wave measurements. Slightly adapting their diffusion coefficient at low $L < 4$ to use a more simple L variation similar to the electrostatic coefficient of *Brautigam and Albert* [2000], one gets approximately

$$D_{LL}\ (\mathrm{day}^{-1}) \simeq D_{LL}^0 \cdot L^6,\ D_{LL}^0 \simeq 10^{-7+0.46K_p},\ L \sim 2 - 4 \tag{A1}$$

during low to high geomagnetic activity periods such that $K_p < 6$. Note that the above diffusion coefficient is independent of electron energy. It stems from the very weak dependence on frequency (and hence electron energy under the action of drift resonant diffusion) of the ULF wave electric field power at frequencies

$\sim 1-10$ mHz for $L = 2.5-4.5$ [*Ozeke et al.*, 2014]. It has also been checked that these new D_{LL} coefficients produce a radial diffusion of energetic electrons in reasonable agreement with observations at $L \sim 2-5$ [*Ozeke et al.*, 2014]. In the present work, the more straightforward formulation given in (A1) will be used to simplify the analytical estimates.

Appendix B: Analytical Estimates of Relativistic Electron Lifetimes at $L \sim 1.5-4$ Inside the Plasmasphere

We only consider here estimates valid when cyclotron resonance with hiss waves dominates pitch angle scattering toward the loss cone. When hiss waves are present alone, such a prevalence of cyclotron resonance scattering requires that $p(\Omega_{pe0}/\Omega_{ce0})\sqrt{\omega_m/\Omega_{ce0}} > 2$ and $p\tan^{2/5}\Delta\theta\Omega_{pe0}\omega_m^{3/2}/\Omega_{ce0}^{5/2} > 0.23$ [*Mourenas et al.*, 2012b; *Artemyev et al.*, 2013b], corresponding to electrons of high enough energy $E > E_{\min}$ (with p the normalized momentum, Ω_{ce0} and Ω_{pe0} the equatorial gyrofrequency and plasma frequency, ω_m the wave mean angular frequency, and $\Delta\theta$ the wave normal angle width of the wave Gaussian distribution). The additional existence of higher-frequency lightning-generated, VLF, or fast magnetosonic waves generally relaxes the second condition for $E > 1-2$ MeV electrons at $L < 3$ [*Artemyev et al.*, 2013b; *Agapitov et al.*, 2014; *Meredith et al.*, 2009; *Mourenas et al.*, 2013], giving finally $E_{\min} \sim 3.5(2/L)^{2.9}$ MeV for a nearly constant mean hiss frequency $f_m \sim 350$ Hz and a typical plasmaspheric density profile [*Ozhogin et al.*, 2012; *Meredith et al.*, 2007].

In such a situation, the loss time scale τ_L can be written approximately as (for details of the derivation, see *Mourenas and Ripoll* [2012], *Mourenas et al.* [2012b], and *Artemyev et al.* [2013b])

$$\tau_L\ (\text{day}) \sim \frac{p^{3/2}\gamma\omega_m^{7/9}\Omega_{pe0}^{14/9}\ln(1/\sin\alpha_{LC})}{2000(\text{rad}\cdot\text{pT}^{-2}\cdot\text{s}^{-1}\cdot\text{day}^{-1})B_w^2\Omega_{ce0}^{12/9}} \tag{B1}$$

with α_{LC} the equatorial loss cone angle, γ the Lorentz factor, and B_w the average magnetic amplitude (in pT) of the waves. Electron lifetimes vary roughly like $p^{3/2}\gamma L^{2.6}/B_w(L)^2$; they are almost independent of both the wave bandwidth $\Delta\omega$ and the wave normal angle width $\Delta\theta \approx 45°$ (see scaling laws in *Mourenas et al.*, [2012b] and *Artemyev et al.* [2013b]).

Comprehensive wave statistics from Akebono and CRRES satellites have provided the needed magnetic local time and bounce-averaged root-mean-square amplitudes of plasmaspheric hiss (between about 0.1 and 1.5 kHz) over $L \sim 1.5$ to 4 during moderately active periods with $K_p < 3$ [*Meredith et al.*, 2007; *Agapitov et al.*, 2014]. Such statistics are in rough agreement with more recent measurements from the Van Allen Probes and Time History of Events and Macroscale Interactions during Substorms satellites between September 2012 and October 2013 over $L \sim 1.5$ to 5 [*Thorne et al.*, 2013a; *Baker et al.*, 2014]. For the sake of simplicity, we shall use here a linear fit $B_w \approx 28(L/3.4)^{1/2}$ pT, representing a good compromise between old and new statistics over $L \sim 1.75-4$.

Appendix C: Approximate Analytical Solution for Inward Radial Diffusion From a Preexisting Flux Peak at $L_0 \sim 2.5-4$

Since radial diffusion of high pitch angle relativistic electrons occurs almost independently of pitch angle scattering in our case, we can first look for a simplified analytical solution $f \sim F_L$ to equation (1) with infinite lifetime τ_L.

Examining equation (1), it is plain to see that its mathematical form is very similar to the form of the one-dimensional equation describing energy diffusion of particles by whistler-mode waves [e.g., see *Balikhin et al.*, 2012; *Mourenas et al.*, 2015, and references therein]. In the latter case, a simplified analytical formulation assuming *energy broadening* of an initially cold distribution has been shown to represent a good approximation of the full solution in various cases [*Mourenas et al.*, 2015].

Actually, the production of enhanced energetic electron populations often occurs at $L_0 \leq 4$ during periods of increased geomagnetic activity just outside of the eroded plasmasphere [e.g., see *Horne et al.*, 2005; *Li et al.*, 2006; *Baker et al.*, 2013; *Thorne et al.*, 2013a; *Zhao and Li*, 2013a; *Li et al.*, 2014a]. We make the further conjecture that the plasmasphere subsequently inflates more quickly (over a time scale of a few days) than both wave-induced losses and radial diffusion, as frequently observed. Although the first flux maximum produced by a given storm is usually broad in L, the close occurrence of a subsequent, weaker disturbance, or strong

wave-induced losses nearby an outward moving plasmapause [*Thorne*, 2010; *Shprits et al.*, 2013; *Usanova et al.*, 2014; *Ma et al.*, 2015] and enhanced outward radial transport [*Shprits et al.*, 2008; *Turner et al.*, 2012; *Ukhorskiy et al.*, 2015] can concur to produce a rapid decrease of $f(L)$ at higher L and consequently a significant narrowing of the flux peak. Incidentally, it is worth noting that the presence of a large gradient in the electron distribution toward lower L generally allows an easier penetration of relativistic electrons to very low L shells [*Zhao and Li*, 2013a]. Such narrow flux peaks therefore represent very good role models for studying the eventual access of relativistic electrons into the inner belt.

Looking now for an approximate analytical solution $f = F_L(L,t)$ to equation (1) without second term, any acceptable solution should retain at least four basic properties: (i) it should yield a Dirac distribution at $L = L_0$ for $t = 0$ (i.e., the assumed initial condition), (ii) its behavior at $t > 0$ and $L < L_0$ should correspond to the spatial broadening of an initial Dirac-like distribution in L_0 analogous to the general (energy-broadening) solution of an energy (or heat) equation of a similar type, (iii) it should reduce to the same form as the exact solution in some limit (for instance for $L_0 = 0$), and (iv) the corresponding phase space density (PSD) integrated over L should be (nearly) conserved over time; i.e., the total number of particles should remain nearly constant. The above four conditions should ensure that the approximate solution retains at least the general shape of the exact one over all the considered parameter range.

Accordingly, the approximate solution $f = F_L(L,t)$ (at fixed adiabatic invariant $M \sim \zeta$) is assumed to take the classical general form corresponding to the diffusive broadening of an initially narrow distribution [e.g., see *Balikhin et al.*, 2012; *Mourenas et al.*, 2015]

$$F_L(L,t) \sim \frac{1}{t^C} \exp\left(-\frac{G(L)}{AD_{LL}^0 L^6\, t}\right) \tag{C1}$$

for $L < L_0 \leq 4$, where D_{LL}^0 is equal to D_{LL} evaluated at $L = 1$, A and C are numerical constants to be determined, and $G(L)$ is a function of L which must also be determined. Substituting the above expression for $F_L(L,t)$ in equation (1) with infinite lifetimes and equating separately the terms in $1/t$ and $1/(D_{LL}t^2)$ on the left- and right-hand sides, one obtains a set of two coupled equations for $G(L)$, A, and C:

$$\begin{aligned} AG &= \left(\frac{\partial G}{\partial L}\right)^2 + \frac{36G^2}{L^2} - \frac{12G}{L}\frac{\partial G}{\partial L} \\ AC &= \frac{\partial^2 G}{\partial L^2} - \frac{17}{2L}\frac{\partial G}{\partial L} + \frac{21G}{L^2} \end{aligned} \tag{C2}$$

The above system of equations does not seem to have exact analytical solutions, except in the trivial case $L_0 = 0$ leading to $G(L) = L^2$, $A = 16$, and $C = 1/4$ in equation (C1). Thus, we have sought *approximate solutions* with G taking the form of a simple analytical function $G = (L_0 - L)(L + BL_0)$ satisfying the above conditions (i)–(iii). In the realistic case $L_0 > 2$, $G(L)$ should indeed be proportional to $(L_0 - L)$ (to some power) in order to become null at $L = L_0$ to satisfy the above conditions (i)–(iii).

Since we aim at addressing the question of inward diffusion of relativistic electrons toward the inner radiation belt, we shall hereafter focus on the domain $L \leq L_0$. We have tried various values for B. For very small $0 \leq (L_0 - L) < 0.2$, a good solution is $G = (L - L_0)^2$, $A \sim 4$, $C \sim 1/2$. But over the much wider and more useful parameter range $(L_0 - L) \sim 0.13 - 1.3$, the approximate solution allowing to satisfy system (C2) most accurately for $2.5 \leq L_0 \leq 4$ appears to be

$$G = L(L_0 - L)\ , A \simeq 23.6\ , C \simeq 0.5 \tag{C3}$$

The latter average values of A and C have been checked to remain generally within about 35% of the exact values given by (C2) over the considered parameter range. Figure C1 further shows that the above approximate coefficient A remains within only $\sim$ 15% of the exact one for $0.17 \leq (L_0 - L) \leq 1.25$. The approximate coefficient $C \sim 1/2$ for $G = (L_0 - L)L$ from (C3) also happens to coincide with the exact one obtained when $L \simeq L_0$ for $G = (L - L_0)^2$ (the latter constituting a more accurate solution when $(L_0 - L) < 0.2$). For low values of $(L_0 - L) \leq 0.1$, the exponent in equation (C1) actually becomes small for reasonable values of $t \geq t_{\min}(L) \simeq 0.003/(D_{LL}^0 L^5)$, where $t_{\min}(L = 3) \sim 20$ days for $K_p \sim 1.5$. For $t \geq t_{\min}(L)$, the sensible underestimation of the exact value of A entailed by the use of (C3) when $(L_0 - L) \leq 0.10$ has therefore little incidence on the level of F_L.

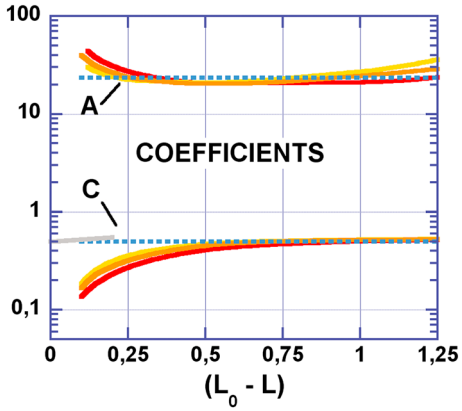

Figure C1. Exact coefficients A and C for F_L obtained by numerically solving the system (C2) with $G = L(L_0 - L)$. The upper and lower curves show A and C, respectively, for $L_0 = 4$ (red), $L_0 = 3$ (orange), and $L_0 = 2.5$ (yellow). The exact coefficient C obtained with $G = (L - L_0)^2$ over its range of applicability $0 \leq (L0 - L) < 0.2$ is also plotted (grey curve). The corresponding approximations given in equation (C3) are displayed over their range of applicability $0.1 < (L_0 - L) < 1.25$ (dotted blue lines).

Moreover, the magnitude of the error on A (and C) is *much smaller* than the intrinsic uncertainty on the actual value of D_{LL} inferred from measurements, which is typically a factor of ~ 3 [e.g., see *Ozeke et al.*, 2012, 2014]. Equations (C1) and (C3) therefore provide a reasonably accurate simplified analytical solution for the electron distribution produced by inward radial diffusion from a preexisting narrow flux peak at $L \sim L_0$. Furthermore, this approximate solution also fulfils the additional condition (iv) listed above: the corresponding phase space density integrated over L is nearly conserved over time. For instance, we have checked numerically that the integral of $F_L(L,t)$ between $L \sim 1$ and $L = L_0 = 3$ is conserved within $\sim$30% when t varies between $t = 1.3t_{\min}(L_0)$ and $t = 8t_{\min}(L_0)$. Physically, it means that the total number of particles is conserved—a required property for any realistic approximate solution.

Appendix D: Details of Application of the Proposed Methods

As discussed in section 4.1, when a maximum of electron PSD (at high equatorial pitch angle $\alpha_0 > 70°$) exists at $L < 4$ in the plasmasphere with a steep decreasing slope toward lower L, the simplified analytical formulations provided in this paper can be used to determine the parameter domains wherein radial diffusion or losses to the atmosphere dominate the evolution of the electron PSD measured by satellite. To this aim, the following successive operations have to be carried out:

1. Determine the average value of K_p over the considered time period and deduce from it the average value of D_{LL}^0 from equation (A1);
2. Determine the equatorial electron plasma frequency profile $\Omega_{pe0}(L)$, the average intensity $B_w^2(L)$ and mean frequency $\omega_m(L)$ profiles for hiss waves (either from statistics or directly measured during this period) and evaluate electron lifetime $\tau_L(L)$ from equation (B1) for a given electron energy E, then substitute into the latter expression $p(M,L) \rightarrow (L_0/L)^{3/2} p(M, L = L_0)$ to get the lifetime $\tau_L(M,L)$ for fixed adiabatic invariant M;
3. Choose a value of $t = t_0 \geq t_{\min}(L) = 0.003/(D_{LL}^0 L^5)$ (taking in the latter inequality the minimum considered L value);
4. Select a value L_0 of L such that the measured $f(L,t_0)$ decreases steeply for $L \leq L_0$ and the measured $f(L,t_0)$ nearly reaches its maximum at $L = L_0$ (L_0 should therefore be lower than, or equal to, the L position of the actual maximum);
5. Adjust slightly t_0 and L_0 values to get with equation (2) for f (multiplied by an appropriate constant normalization factor and using D_{LL}^0 and $\tau_L(M,L)$ determined above) the best possible fit to the measured $f(L,t_0)$ at $L \leq L_0$; and
6. The parameter domain of dominating lossless radial diffusion corresponds to (E,L,t) or (M,L,t) regions where $t < \min(t_{\max}, \tau_L/3)$ with $t_{\max}(M,L)$ given by equation (3); conversely, if $t > \min(t_{\max}, \tau_L/3)$, we are in a loss-limited regime of radial diffusion (the latter domain is also given more approximately by equation (4)). Measured electron PSD decay time scales should correspond to lifetimes τ_L only when $t > 2t_{\max}(M,L)$.

To infer D_{LL}^0 values from measured electron PSD (as in section 4.3), one should first carry out the same operations 1 to 5 listed above, and then (1) select a L value such that $(L_0 - L) \geq 0.5$, times t_1 and t_2 such that $t_2/t_1 \sim 2-4$, and a high electron energy $E > 3$ MeV, and (2) the value of D_{LL}^0 can be obtained from equation (9).

References

Abel, B., R. M. Thorne, and A. L. Vampola (1997), Energetic electron precipitation from the inner zone, *Geophys. Res. Lett.*, *24*, 1983–1986, doi:10.1029/97GL02055.

Agapitov, O., A. Artemyev, V. Krasnoselskikh, Y. V. Khotyaintsev, D. Mourenas, H. Breuillard, M. Balikhin, and G. Rolland (2013), Statistics of Whistler-Mode Waves in the Outer Radiation Belt: Cluster STAFF-SA measurements, *J. Geophys. Res. Space Physics*, *118*, 3407–3420, doi:10.1002/jgra.50312.

Acknowledgments
The Van Allen Probes data used are publicly available at www.rbsp-ect.lanl.gov. All the other new data used in this paper are obtained from analytical formulas provided here. Corresponding parameters and boundary conditions are listed in the text. The 3 h K_p index can be obtained from the GFZ German Research Center for Geosciences at ftp://ftp.gfz-potsdam.de/pub/home/obs/kp-ap/. We also would like to thank V. Krasnoselskikh for useful discussions.

Michael Liemohn thanks the reviewers for their assistance in evaluating this paper.

Agapitov, O., A. Artemyev, D. Mourenas, Y. Kasahara, and V. Krasnoselskikh (2014), Inner belt and slot region electron lifetimes and energization rates based on AKEBONO statistics of whistler waves, *J. Geophys. Res. Space Physics*, *119*, 2876–2893, doi:10.1002/2014JA019886.

Artemyev, A., O. Agapitov, D. Mourenas, V. Krasnoselskikh, and L. Zelenyi (2013a), Storm-induced energization of radiation belt electrons: Effect of wave obliquity, *Geophys. Res. Lett.*, *40*, 4138–4143, doi:10.1002/grl.50837.

Artemyev, A., D. Mourenas, O. Agapitov, and V. Krasnoselskikh (2013b), Parametric validations of analytical lifetime estimates for radiation belt electron diffusion by whistler waves, *Ann. Geophys.*, *31*, 599–624, doi:10.5194/angeo-31-599-2013.

Baker, D. N., S. G. Kanekal, X. Li, S. P. Monk, J. Goldstein, and J. L. Burch (2004), An extreme distortion of the Van Allen belt arising from the 'Halloween' solar storm in 2003, *Nature*, *432*, 878–881, doi:10.1038/nature03116.

Baker, D. N., et al. (2013), A long-lived relativistic electron storage ring embedded in earths outer Van Allen Belt, *Science*, *340*, 186–190, doi:10.1126/science.1233518.

Baker, D. N., et al. (2014), An impenetrable barrier to ultrarelativistic electrons in the Van Allen radiation belts, *Nature*, *515*, 531–534, doi:10.1038/nature13956.

Balikhin, M. A., M. Gedalin, G. D. Reeves, R. J. Boynton, and S. A. Billings (2012), Time scaling of the electron flux increase at GEO: The local energy diffusion model vs observations, *J. Geophys. Res.*, *117*, A10208, doi:10.1029/2012JA018114.

Blake, J. B., W. A. Kolasinski, R. W. Fillius, and E. G. Mullen (1992), Injection of electrons and protons with energies of tens of MeV into $L < 3$ on March 24 1991, *Geophys. Res. Lett.*, *19*, 821–824, doi:10.1029/92GL00624.

Bortnik, J., L. Chen, W. Li, R. M. Thorne, N. P. Meredith, and R. B. Horne (2011), Modeling the wave power distribution and characteristics of plasmaspheric hiss, *J. Geophys. Res.*, *116*, A12209, doi:10.1029/2011JA016862.

Brautigam, D. H., and J. M. Albert (2000), Radial diffusion analysis of outer radiation belt electrons during the October 9, 1990, magnetic storm, *J. Geophys. Res.*, *105*, 291–309, doi:10.1029/1999JA900344.

Chen, L., W. Li, J. Bortnik, and R. M. Thorne (2012), Amplification of whistler mode hiss inside the plasmasphere, *Geophys. Res. Lett.*, *39*, L08111, doi:10.1029/2012GL051488.

Chiu, Y. T., R. W. Nightingale, and M. A. Rinaldi (1988), Simultaneous radial and pitch angle diffusion in the outer electron radiation belt, *J. Geophys. Res.*, *93*(A4), 2619–2632, doi:10.1029/JA093iA04p02619.

Falthammar, C. G. (1965), Effects of time-dependent electric fields on geomagnetically trapped radiation, *J. Geophys. Res.*, *70*(11), 2503–2516, doi:10.1029/JZ070i011p02503.

Fennell, J. F., S. G. Claudepierre, J. B. Blake, T. P. O'Brien, J. H. Clemmons, D. N. Baker, H. E. Spence, and G. D. Reeves (2015), Van Allen Probes show the inner radiation zone contains no MeV electrons: ECT/MagEIS data, *Geophys. Res. Lett.*, *42*, 1283–1289, doi:10.1002/2014GL062874.

Gabrielse, C., V. Angelopoulos, A. Runov, and D. L. Turner (2012), The effects of transient, localized electric fields on equatorial electron acceleration and transport toward the inner magnetosphere, *J. Geophys. Res.*, *117*, A10213, doi:10.1029/2012JA017873.

Glauert, S. A., R. B. Horne, and N. P. Meredith (2014), Three-dimensional electron radiation belt simulations using the BAS Radiation Belt Model with new diffusion models for chorus, plasmaspheric hiss, and lightning-generated whistlers, *J. Geophys. Res. Space Physics*, *119*, 268–289, doi:10.1002/2013JA019281.

Gubby, R., and J. Evans (2002), Space environment effects and satellite design, *J. Atmos. Sol. Terr. Phys.*, *64*, 1723–1733, doi:10.1016/S1364-6826(02)00122-0.

Horne, R. B., R. M. Thorne, S. A. Glauert, J. M. Albert, N. P. Meredith, and R. R. Anderson (2005), Timescale for radiation belt electron acceleration by whistler mode chorus waves, *J. Geophys. Res.*, *110*, A03225, doi:10.1029/2004JA010811.

Horne, R. B., S. A. Glauert, N. P. Meredith, D. Boscher, V. Maget, D. Heynderickx, and D. Pitchford (2013), Space weather impacts on satellites and forecasting the Earth's electron radiation belts with SPACECAST, *Space Weather*, *11*, 169–186, doi:10.1002/swe.20023.

Kennel, C. F., and H. E. Petschek (1966), Limit on stably trapped particle fluxes, *J. Geophys. Res.*, *71*, 1–28, doi:10.1029/JZ071i001p00001.

Kellerman, A. C., Y. Y. Shprits, D. Kondrashov, D. Subbotin, R. A. Makarevich, E. Donovan, and T. Nagai (2014), Three-dimensional data assimilation and reanalysis of radiation belt electrons: Observations of a four-zone structure using five spacecraft and the VERB code, *J. Geophys. Res. Space Physics*, *119*, 8764–8783, doi:10.1002/2014JA020171.

Kim, K.-C., and Y. Shprits (2012), Radial gradients of phase space density in the inner electron radiation, *J. Geophys. Res.*, *117*, A12209, doi:10.1029/2012JA018211.

Li, X., I. Roth, M. Temerin, J. R. Wygant, M. K. Hudson, and J. B. Blake (1993), Simulation of the prompt energization and transport of radiation particles during the March 24 1991 SSC, *Geophys. Res. Lett.*, *20*, 2423–2426, doi:10.1029/93GL02701.

Li, X., D. N. Baker, S. G. Kanekal, M. Looper, and M. Temerin (2001), Long term measurements of radiation belts by SAMPEX and their variations, *Geophys. Res. Lett.*, *28*, 3827–3830, doi:10.1029/2001GL013586.

Li, X., D. N. Baker, T. P. O'Brien, L. Xie, and Q. G. Zong (2006), Correlation between the inner edge of outer radiation belt electrons and the innermost plasmapause location, *Geophys. Res. Lett.*, *33*, L14107, doi:10.1029/2006GL026294.

Li, X., R. S. Selesnick, D. N. Baker, A. N. Jaynes, S. G. Kanekal, Q. Schiller, L. Blum, J. Fennell, and J. B. Blake (2015), Upper limit on the inner radiation belt MeV electron intensity, *J. Geophys. Res. Space Physics*, *120*, 1215–1228, doi:10.1002/2014JA020777.

Li, W., B. Ni, R. M. Thorne, J. Bortnik, J. C. Green, C. A. Kletzing, W. S. Kurth, and G. B. Hospodarsky (2013), Constructing the global distribution of chorus wave intensity using measurements of electrons by the POES satellites and waves by the Van Allen Probes, *Geophys. Res. Lett.*, *40*, 4526–4532, doi:10.1002/grl.50920.

Li, W., et al. (2014a), Radiation belt electron acceleration by chorus waves during the 17 March 2013 storm, *J. Geophys. Res. Space Physics*, *119*, 4681–4693, doi:10.1002/2014JA019945.

Li, W., et al. (2014b), Evidence of stronger pitch angle scattering loss caused by oblique whistler-mode waves as compared with quasi-parallel waves, *Geophys. Res. Lett.*, *41*, 6063–6070, doi:10.1002/2014GL061260.

Livadiotis, G. (2015), Statistical background and properties of Kappa distributions in space plasmas, *J. Geophys. Res. Space Physics*, *120*, 1607–1619, doi:10.1002/2014JA020825.

Looper, M. D., J. B. Blake, and R. A. Mewaldt (2005), Response of the inner radiation belt to the violent Sun-Earth connection events of OctoberŰNovember 2003, *Geophys. Res. Lett.*, *32*, L03S06, doi:10.1029/2004GL021502.

Lyons, L. R., and R. M. Thorne (1973), Equilibrium structure of radiation belt electrons, *J. Geophys. Res.*, *78*, 2142–2149, doi:10.1029/JA078i013p02142.

Lyons, L. R., R. M. Thorne, and C. F. Kennel (1972), Pitch-angle diffusion of radiation belt electrons within the plasmasphere, *J. Geophys. Res.*, *77*, 3455–3474, doi:10.1029/JA077i019p03455.

Ma, Q., et al. (2015), Modeling inward diffusion and slow decay of energetic electrons in the Earth's outer radiation belt, *Geophys. Res. Lett.*, *42*, 987–995, doi:10.1002/2014GL062977.

Meredith, N. P., R. B. Horne, S. A. Glauert, and R. R. Anderson (2007), Slot region electron loss timescales due to plasmaspheric hiss and lightning-generated whistlers, *J. Geophys. Res.*, *112*, A08214, doi:10.1029/2007JA012413.

Meredith, N. P., R. B. Horne, S. A. Glauert, D. N. Baker, S. G. Kanekal, and J. M. Albert (2009), Relativistic electron loss timescales in the slot region, *J. Geophys. Res.*, *114*, A03222, doi:10.1029/2008JA013889.

Meredith, N. P., R. B. Horne, A. Sicard-Piet, D. Boscher, K. H. Yearby, W. Li, and R. M. Thorne (2012), Global model of lower band and upper band chorus from multiple satellite observations, *J. Geophys. Res.*, *117*, A10225, doi:10.1029/2012JA017978.

Meredith, N. P., R. B. Horne, T. Kersten, B. J. Fraser, and R. S. Grew (2014), Global morphology and spectral properties of EMIC waves derived from CRRES observations, *J. Geophys. Res. Space Physics*, *119*, 5328–5342, doi:10.1002/2014JA020064.

Mourenas, D., and J. F. Ripoll (2012), Analytical estimates of quasi-linear diffusion coefficients and electron lifetimes in the inner radiation belt, *J. Geophys. Res.*, *117*, A01204, doi:10.1029/2011JA016985.

Mourenas, D., A. Artemyev, O. Agapitov, and V. Krasnoselskikh (2012a), Acceleration of radiation belts electrons by oblique chorus waves, *J. Geophys. Res.*, *117*, A10212, doi:10.1029/2012JA018041.

Mourenas, D., A. V. Artemyev, J.-F. Ripoll, O. V. Agapitov, and V. V. Krasnoselskikh (2012b), Timescales for electron quasi-linear diffusion by parallel and oblique lower-band Chorus waves, *J. Geophys. Res.*, *117*, A06234, doi:10.1029/2012JA017717.

Mourenas, D., A. V. Artemyev, O. V. Agapitov, and V. V. Krasnoselskikh (2013), Analytical estimates of electron quasi-linear diffusion by fast magnetosonic waves, *J. Geophys. Res. Space Physics*, *118*, 3096–3112, doi:10.1002/jgra.50349.

Mourenas, D., A. Artemyev, O. Agapitov, and V. Krasnoselskikh (2014), Consequences of geomagnetic activity on energization and loss of radiation belt electrons by oblique chorus waves, *J. Geophys. Res. Space Physics*, *119*, 2775–2796, doi:10.1002/2013JA019674.

Mourenas, D., A. Artemyev, O. Agapitov, V. Krasnoselskikh, and W. Li (2015), Approximate analytical solutions for the trapped electron distribution due to quasi-linear diffusion by whistler-mode waves, *J. Geophys. Res. Space Physics*, *119*, 9962–9977, doi:10.1002/2014JA020443.

Ni, B., J. Bortnik, R. M. Thorne, Q. Ma, and L. Chen (2013), Resonant scattering and resultant pitch angle evolution of relativistic electrons by plasmaspheric hiss, *J. Geophys. Res. Space Physics*, *118*, 7740–7751, doi:10.1002/2013JA019260.

Ni, B., et al. (2015), Variability of the pitch-angle distribution of radiation belt electrons during and following intense geomagnetic storms: Van Allen Probes observations, *J. Geophys. Res. Space Physics*, *120*, 4863–4876, doi:10.1002/2015JA021065.

O'Brien, T. P., and M. B. Moldwin (2003), Empirical plasmapause models from magnetic indices, *Geophys. Res. Lett.*, *30*(4), 1152, doi:10.1029/2002GL016007.

O'Brien, T. P., K. R. Lorentzen, I. R. Mann, N. P. Meredith, J. B. Blake, J. F. Fennell, M. D. Looper, D. K. Milling, and R. R. Anderson (2003), Energization of relativistic electrons in the presence of ULF power and MeV microbursts: Evidence for dual ULF and VLF acceleration, *J. Geophys. Res.*, *108*(A8), 1329, doi:10.1029/2002JA009784.

Ozeke, L. G., I. R. Mann, K. R. Murphy, I. J. Rae, D. K. Milling, S. R. Elkington, A. A. Chan, and H. J. Singer (2012), ULF wave derived radiation belt radial diffusion coefficients, *J. Geophys. Res.*, *117*, A04222, doi:10.1029/2011JA017463.

Ozeke, L. G., I. R. Mann, K. R. Murphy, I. Jonathan Rae, and D. K. Milling (2014), Analytic expressions for ULF wave radiation belt radial diffusion coefficients, *J. Geophys. Res. Space Physics*, *119*, 251–258, doi:10.1002/2013JA019204.

Ozhogin, P., J. Tu, P. Song, and B. W. Reinisch (2012), Field-aligned distribution of the plasmaspheric electron density: An empirical model derived from the IMAGE RPI measurements, *J. Geophys. Res.*, *117*, A06225, doi:10.1029/2011JA017330.

Schulz, M. (1991), The magnetosphere, in *Geomagnetism*, vol. IV, edited by J. A. Jacobs, pp. 87–293, Acad. Press Limited, San Diego, Calif.

Schulz, M., and L. J. Lanzerotti (1974), *Particle Diffusion in the Radiation Belts*, Springer, New York.

Schulz, M., and A. L. Newman (1988), Eigenfunctions of the magnetospheric radial-diffusion operator, *Phys. Scr.*, *37*(4), 632–639, doi:10.1029/JA077i019p03441.

Shprits, Y. Y., and R. M. Thorne (2004), Time dependent radial diffusion modeling of relativistic electrons with realistic loss rates, *Geophys. Res. Lett.*, *31*, L08805, doi:10.1029/2004GL019591.

Shprits, Y. Y., R. M. Thorne, R. B. Horne, S. A. Glauert, M. Cartwright, C. T. Russell, D. N. Baker, and S. G. Kanekal (2006), Acceleration mechanism responsible for the formation of the new radiation belt during the 2003 Halloween solar storm, *Geophys. Res. Lett.*, *33*, L05104, doi:10.1029/2005GL024256.

Shprits, Y. Y., S. R. Elkington, N. P. Meredith, and D. A. Subbotin (2008), Review of modeling of losses and sources of relativistic electrons in the outer radiation belt I: Radial transport, *J. Atmos. Sol. Terr. Phys.*, *70*, 1679–1693, doi:10.1016/j.jastp.2008.06.008.

Shprits, Y. Y., D. Subbotin, A. Drozdov, M. E. Usanova, A. Kellerman, K. Orlova, D. N. Baker, D. L. Turner, and K.-C. Kim (2013), Unusual stable trapping of the ultrarelativistic electrons in the Van Allen radiation belts, *Nat. Phys.*, *9*, 699–703, doi:10.1038/NPHYS2760.

Sicard-Piet, A., D. Boscher, R. B. Horne, N. P. Meredith, and V. Maget (2014), Effect of plasma density on diffusion rates due to wave particle interactions with chorus and plasmaspheric hiss: Extreme event analysis, *Ann. Geophys.*, *32*, 1059–1071, doi:10.5194/angeo-32-1059-2014.

Su, Z., F. Xiao, H. Zheng, and S. Wang (2010), Combined radial diffusion and adiabatic transport of radiation belt electrons with arbitrary pitch angles, *J. Geophys. Res.*, *115*, A10249, doi:10.1029/2010JA015903.

Thorne, R. M. (2010), Radiation belt dynamics: The importance of wave-particle interactions, *Geophys. Res. Lett.*, *372*, L22107, doi:10.1029/2010GL044990.

Thorne, R. M., et al. (2013a), Evolution and slow decay of an unusual narrow ring of relativistic electrons near L 3.2 following the September 2012 magnetic storm, *Geophys. Res. Lett.*, *40*, 3507–3511, doi:10.1002/grl.50627.

Thorne, R. M., et al. (2013b), Rapid local acceleration of relativistic radiation belt electrons by magnetospheric chorus, *Nature*, *504*, 411–414, doi:10.1038/nature12889.

Tomassian, A. D., T. A. Farley, and A. L. Vampola (1972), Inner-zone energetic-electron repopulation by radial diffusion, *J. Geophys. Res.*, *77*(19), 3441–3454, doi:10.1029/JA077i019p03441.

Tu, W., S. R. Elkington, X. Li, W. Liu, and J. Bonnell (2012), Quantifying radial diffusion coefficients of radiation belt electrons based on global MHD simulation and spacecraft measurements, *J. Geophys. Res.*, *117*, A10210, doi:10.1029/2012JA017901.

Tu, W., G. S. Cunningham, Y. Chen, S. K. Morley, G. D. Reeves, J. B. Blake, D. N. Baker, and H. Spence (2014), Event-specific chorus wave and electron seed population models in DREAM3D using the Van Allen Probes, *Geophys. Res. Lett.*, *41*, 1359–1366, doi:10.1002/2013GL058819.

Turner, D. L., Y. Shprits, M. Hartinger, and V. Angelopoulos (2012), Explaining sudden losses of outer radiation belt electrons during geomagnetic storms, *Nat. Phys.*, *8*, 208–212, doi:10.1038/nphys2185.

Ukhorskiy, A. Y., M. I. Sitnov, R. M. Millan, B. T. Kress, J. F. Fennell, S. G. Claudepierre, and R. J. Barnes (2015), Global storm time depletion of the outer electron belt, *J. Geophys. Res. Space Physics*, *120*, 2543–2556, doi:10.1002/2014JA020645.

Usanova, M. E., et al. (2014), Effect of EMIC waves on relativistic and ultrarelativistic electron populations: Ground-based and Van Allen Probes observations, *Geophys. Res. Lett.*, *41*, 1375–1381, doi:10.1002/2013GL059024.

Walt, M. (1970), Radial diffusion of trapped particles, in *Particles and Fields in the Magnetosphere*, edited by B. M. McCormac, p. 410, D. Reidel, Dordrecht, Netherlands.

Wang, Z., Z. Yuan, M. Li, H. Li, D. Wang, H. Li, S. Huang, and Z. Qiao (2014), Statistical characteristics of EMIC wavedriven relativistic electron precipitation with observations of POES satellites: Revisit, *J. Geophys. Res. Space Physics*, *119*, 5509–5519, doi:10.1002/2014JA020082.

West, H. I., Jr. (1966), Some observations of the trapped electrons produced by the Russian high-altitude nuclear detonation of October 28 1962, in *Radiation Trapped in the EarthŠs Magnetic Field*, vol. 634–662, edited by B. M. McCormac, Gordon and Breach, New York.

Xiao, F., C. Shen, Y. Wang, H. Zheng, and S. Wang (2008), Energetic electron distributions fitted with a relativistic kappa-type function at geosynchronous orbit, *J. Geophys. Res.*, *113*, A05203, doi:10.1029/2007JA012903.

Zhao, H., and X. Li (2013a), Inward shift of outer radiation belt electrons as a function of Dst index and the influence of the solar wind on electron injections into the slot region, *J. Geophys. Res. Space Physics*, *118*, 756–764, doi:10.1029/2012JA018179.

Zhao, H., and X. Li (2013b), Modeling energetic electron penetration into the slot region and inner radiation belt, *J. Geophys. Res. Space Physics*, *118*, 6936–6945, doi:10.1002/2013JA019240.

Zhao, H., X. Li, J. B. Blake, J. F. Fennell, S. G. Claudepierre, D. N. Baker, A. N. Jaynes, D. M. Malaspina, and S. G. Kanekal (2014), Peculiar pitch angle distribution of relativistic electrons in the inner radiation belt and slot region, *Geophys. Res. Lett.*, *41*, 2250–2257, doi:10.1002/2014GL059725.

Zhao, H., X. Li, J. B. Blake, J. F. Fennell, S. G. Claudepierre, D. N. Baker, A. N. Jaynes, and D. M. Malaspina (2015), Characteristics of pitch angle distributions of hundreds of keV electrons in the slot region and inner radiation belt, *J. Geophys. Res. Space Physics*, *119*, 9543–9557, doi:10.1002/2014JA020386.